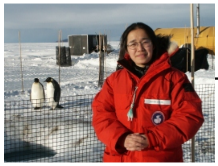

Lecture 17. Temperature Lidar (6) Integration Technique

- ❑ Doppler effects in absorption/backscatter coefficient
- ❑ Integration technique for temperature
  - ➢ Searchlight integration lidar
  - ➢ Rayleigh integration temperature lidar
  - ➢ Vibrational Raman integration lidar
  - ➢ Falling sphere temperature measurement
- ❑ Rayleigh/Raman lidar instrumentation
- ❑ Summary

Doppler Broadening in Absorption and Backscatter Coefficients

- It is accurate to say that absorption coefficient and backscatter coefficient experience Doppler broadening. However, only statistically averaged absorption and effective cross sections experience Doppler broadening.
- Absorption and effective cross sections for single atom/molecule experience Doppler shift but not Doppler broadening.
- Absorption and total backscatter coefficients are given by

$$\alpha_{ik} = \sigma_{ik}\left(N_i - \frac{g_i}{g_k} N_k\right) \approx \sigma_{ik} N_i$$

$$\beta_T = \sigma_{eff} R_B N_i$$

- Absorption coefficient α_{ik}, total backscatter coefficient β_T
- Absorption cross section σ_{ik}, effective backscatter cross section σ_{eff}
- Population (number density) N_i and N_k

Doppler Shift in Absorption and Backscatter Cross Sections

- In principle, σ_{ik} is the cross section for single atom/molecule, so $\sigma_{ik}(\omega)$ has a Lorentzian shape L(ω, V)

$$\sigma_{ik}(\omega,v) = \sigma_o L(\omega,v)$$

where L(ω, v) is a Lorentzian shape and function of velocity v.

- Single atom absorption/effective cross section experiences Doppler shift, but it does NOT experience Doppler broadening. Single atom cross-section has a Lorentzian shape with narrow natural linewidth, resulted from the finite radiative lifetime of the excited states of atom/molecule.

- N_i can be written as the population distribution along velocity $N_i(v)$, which is a Gaussian shape under Maxwellian distribution:

$$N_i(v,V_R) = N_o G(v,V_R)$$

- Doppler broadening comes from the fact that different atoms have different velocities in the atmosphere, so causing different Doppler shifts. Averaging over all atoms, it leads to Doppler broadened Gaussian shape.

Doppler Broadening on Absorption and Backscatter Coefficients

- α_{ik} is the convolution of a Lorentzian absorption cross section with a Gaussian population distribution, which becomes a Voigt profile:

$$\alpha_{ik}(\omega,V_R) = \int_{-\infty}^{+\infty}\sigma_{ik}(\omega,v)N_i(v,V_R)dv = \sigma_o N_o \int_{-\infty}^{+\infty} L(\omega,v)G(v,V_R)dv$$

- But it is common to shift all distribution factors to the absorption cross section, and then N_i will only count the total population.

$$\sigma_{ik,ave} = \sigma_o \int_{-\infty}^{+\infty} L(\omega,v)G(v,V_R)dv$$

- In this case, it is now a cross section for the atom assembly (but normalized to single molecule), not for single molecule anywhere.

About Doppler-free Spectroscopy

- In Doppler-free or sub-Doppler spectroscopy, we have to use single atom/molecule absorption cross section that is Lorentzian with different velocity distributions of population to derive the sub-Doppler feature.
- How to defeat Doppler broadening to achieve Doppler-free spectroscopy? – Choose a subgroup of atom velocity!
- Homogeneous broadening vs. inhomogeneous broadening

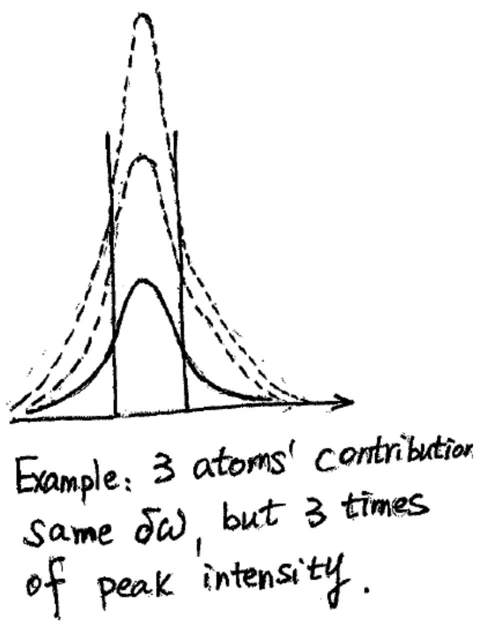

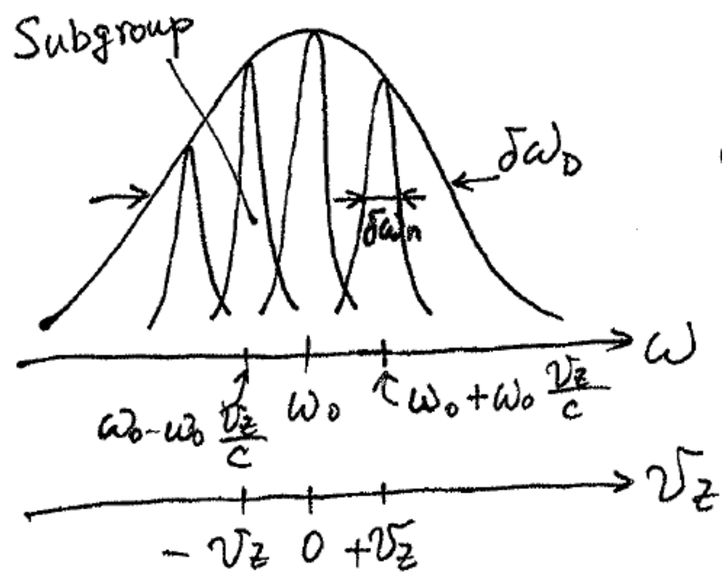

Review of Doppler & Boltzmann

- Doppler effect and Boltzmann distribution are two effects that are directly temperature-dependent. The Doppler technique and Boltzmann technique are "straight-forward" in the sense of deriving temperature or wind. However, the lidar architecture is usually complicated and sophisticated, due to the high demands on frequency accuracy and tuning, laser linewidth, and laser power etc.

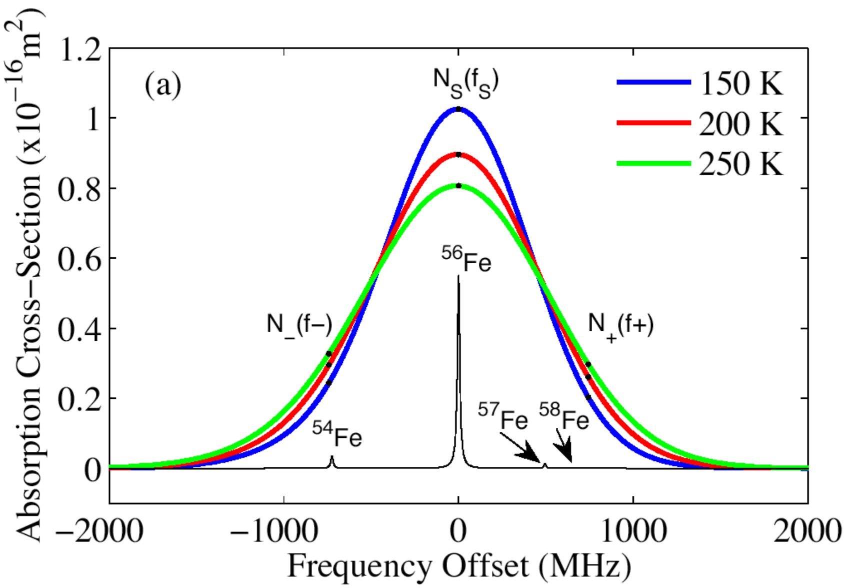

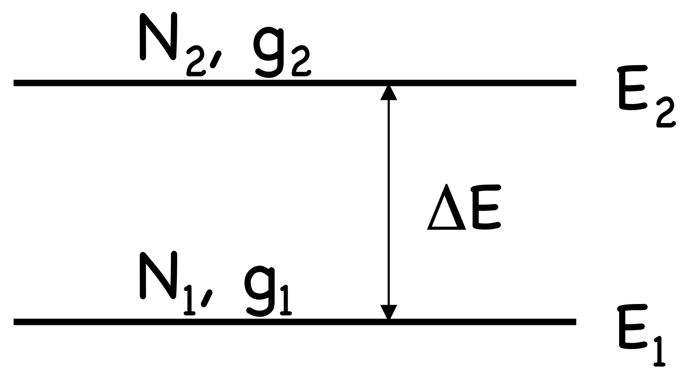

$$\frac{N_2}{N_1} = \frac{g_2}{g_1}\exp\left\{-\left(E_2 - E_1\right)/k_B T\right\}$$

$$\Delta\omega = \omega - \omega_0 = -\vec{k}\cdot\vec{v} = -\omega_0 \frac{v\cos\theta}{c}$$

$$T = \frac{\Delta E / k_B}{\ln\left(\frac{g_2}{g_1}\cdot\frac{N_1}{N_2}\right)}$$

$$\sigma_{rms} = \frac{\nu_0}{c}\sqrt{\frac{k_B T}{M}} = \frac{1}{\lambda_0}\sqrt{\frac{k_B T}{M}}$$

Integration Technique

- The hydrostatic equation

$$dP(z) = -\rho(z)g(z)dz$$

- Ideal gas law

$$P(z) = \frac{\rho(z)RT(z)}{M(z)}$$

- Integration from the upper altitude yields

$$T(z) = T(z_0)\frac{\rho(z_0)}{\rho(z)}\frac{M(z)}{M(z_0)} + \frac{M(z)}{R}\int_z^{z_0}\frac{\rho(z')g(z')}{\rho(z)}dz'$$

$T(z)$ = atmospheric temperature profile (K)

$P(z)$ = atmospheric pressure profile (mbar)

$\rho(z)$ = atmospheric mass density profile (kg/m^3)

$g(z)$ = gravitational acceleration (m/s^2)

$M(z)$ = mean molecular weight of the atmosphere,
i.e., molecular mass per mole (kg/mol)

R = universal gas constant (8.314472 J/mol/K)

z_0 = altitude of the upper level starting temperature (m)

Integration Technique

- Atmosphere mass density $\rho(z)$ vs number density $n(z)$

$$\rho(z) = n(z)M(z)/N_A$$

where N_A is the Avogadro constant: $N_A = 6.02214179\times10^{23}\ \mathrm{mol}^{-1}$

- Thus, we have

$$T(z) = T(z_0)\frac{n(z_0)}{n(z)} + \frac{M(z)}{R}\int_z^{z_0}\frac{n(z')M(z')g(z')}{n(z)M(z)}\,\mathrm{d}z'$$

- Below 100 km for the well-mixed atmosphere, we have M(z) = M(z'), so they cancel out in the integration

$$T(z) = T(z_0)\frac{n(z_0)}{n(z)} + \frac{M(z)}{R}\int_z^{z_0}\frac{n(z')g(z')}{n(z)}\,\mathrm{d}z'$$

- Number density ratio (relative number density)

⇨ Temperature profile

Error Analysis for Integration Tech

- The uncertainty is determined by the photon noise and upper altitude temperature T(z_0). The variance of derived temperature is given by

$$\mathrm{var}[T(z)] \approx \frac{T^2(z)}{N_R(z)} + \left\{ \mathrm{var}[T(z_0)] + \frac{T^2(z_0)}{N_R(z_0)} \right\} \exp\left[-2(z_0 - z)/H\right]$$

- After 1-2 scale height, the error introduced by T(z_0) is not important anymore. So the temperature error is mainly determined by the photon counts and their noise.

- The key is how to measure atmosphere (relative) density with high accuracy and precision. Different approaches can be applied, not limited to pulsed lidar technique.

From Searchlight to Rayleigh, Raman & Falling Sphere

- Integration temperature technique relies on the assumptions of hydrostatic equilibrium equation and ideal gas law in atmosphere. It involves integrating the atmosphere relative density profile downward using a starting temperature at an upper altitude.
- It was pioneered by *Elterman* [1951, 1953, 1954] with cw searchlight to measure stratospheric density thus deriving temperature in 1950s.
- The use of high power lasers with the Rayleigh lidar in the atmosphere region (30-100 km) free of aerosol and fluorescence was pioneered by *Hauchecorne and Chanin* [1980] (French group).
- In the lower atmosphere where aerosol scattering contaminates Rayleigh scattering, *Keckhut et al.* [1990] developed Raman lidar to measure atmosphere density from vibrational Raman scattering and then derive temperature below 30 km.
- Inflatable falling sphere provides high-precision atmosphere density thus temperature measurements [*Schmidlin et al.,* 1991].

Rayleigh, Raman & Falling Sphere using Integration Temperature Technique

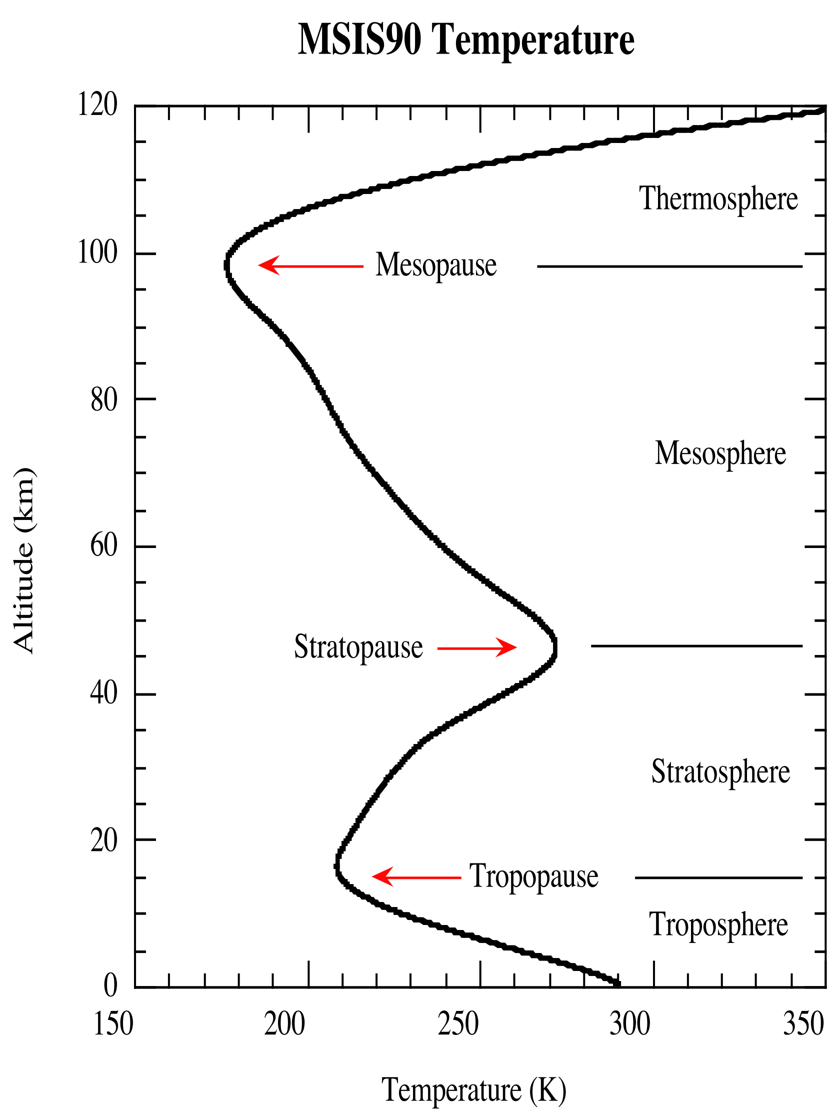

Rayleigh Integration Lidar

Vibrational Raman Lidar

Falling Sphere

Searchlight

Searchlight Integration Lidar

$$I_{scatter} \propto n_{atmos}$$

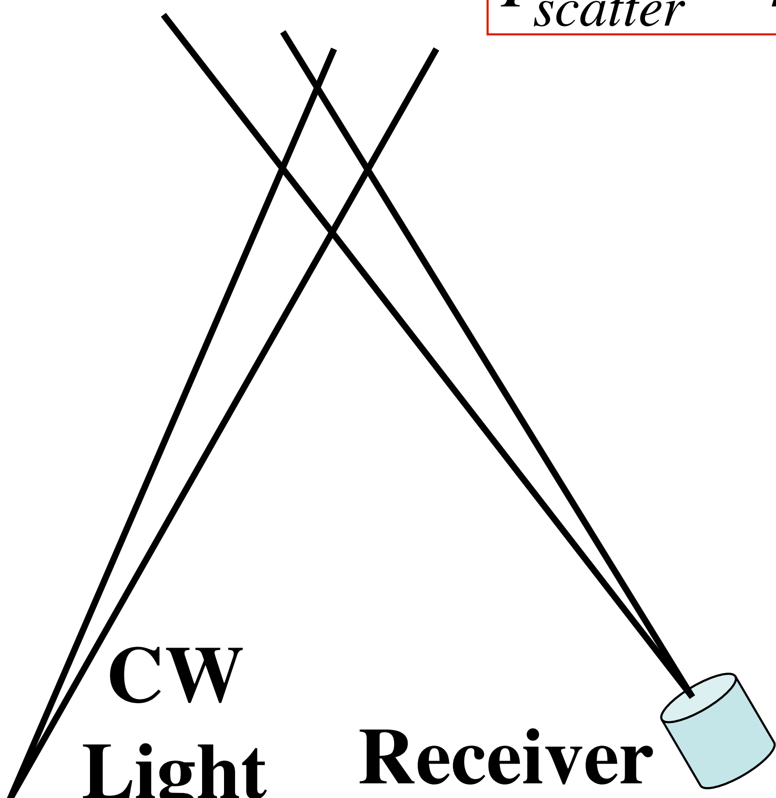

Bistatic Configuration

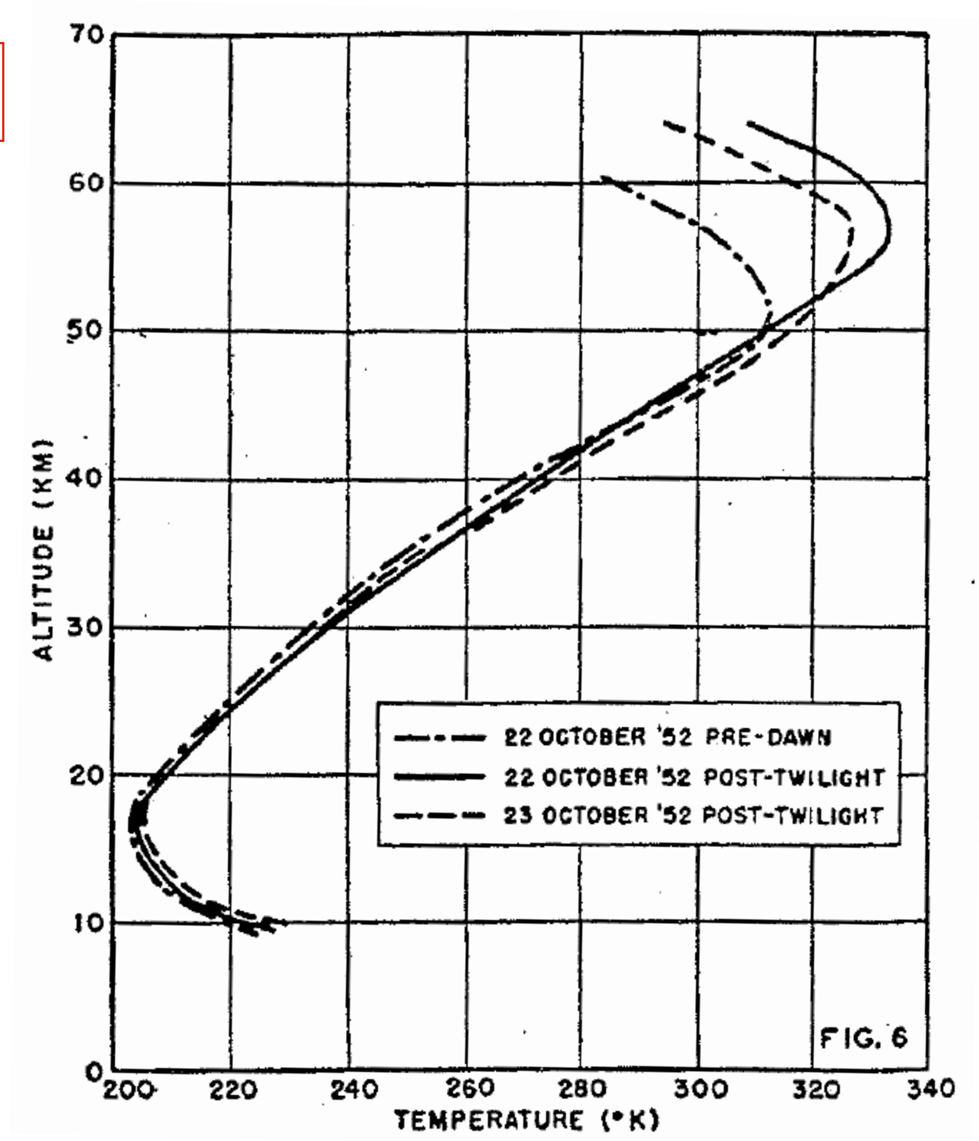

[Elterman, JGR, 1954]

Rayleigh Integration Lidar

- In the atmosphere region free of aerosols and fluorescence, the lidar return photon counts are given by

$$N_S(\lambda,z) = \left(\frac{P_L(\lambda)\Delta t}{hc/\lambda}\right)\left(\beta_{Rayleigh}(z)\Delta z\right)\left(\frac{A}{z^2}\right)T_a{}^2(\lambda,z)\left(\eta(\lambda)G(z)\right) + N_B$$

where Rayleigh backscatter coefficient is proportional to atmosphere number density $\beta_{Ray}(z) = \sigma_{Ray}(\pi,\lambda)n_a(z)$

- Thus, ratio of normalized photon counts gives the atmosphere relative density information

$$\frac{N_S(z_1) - N_B}{N_S(z_2) - N_B}\frac{z_1^2}{z_2^2} = \frac{n_a(z_1)}{n_a(z_2)}$$

Lidar Backscatter Ratio ⇒ Relative Density ⇒ Temperature
(at different altitudes) (Rayleigh)

Sample of Temperature and Error

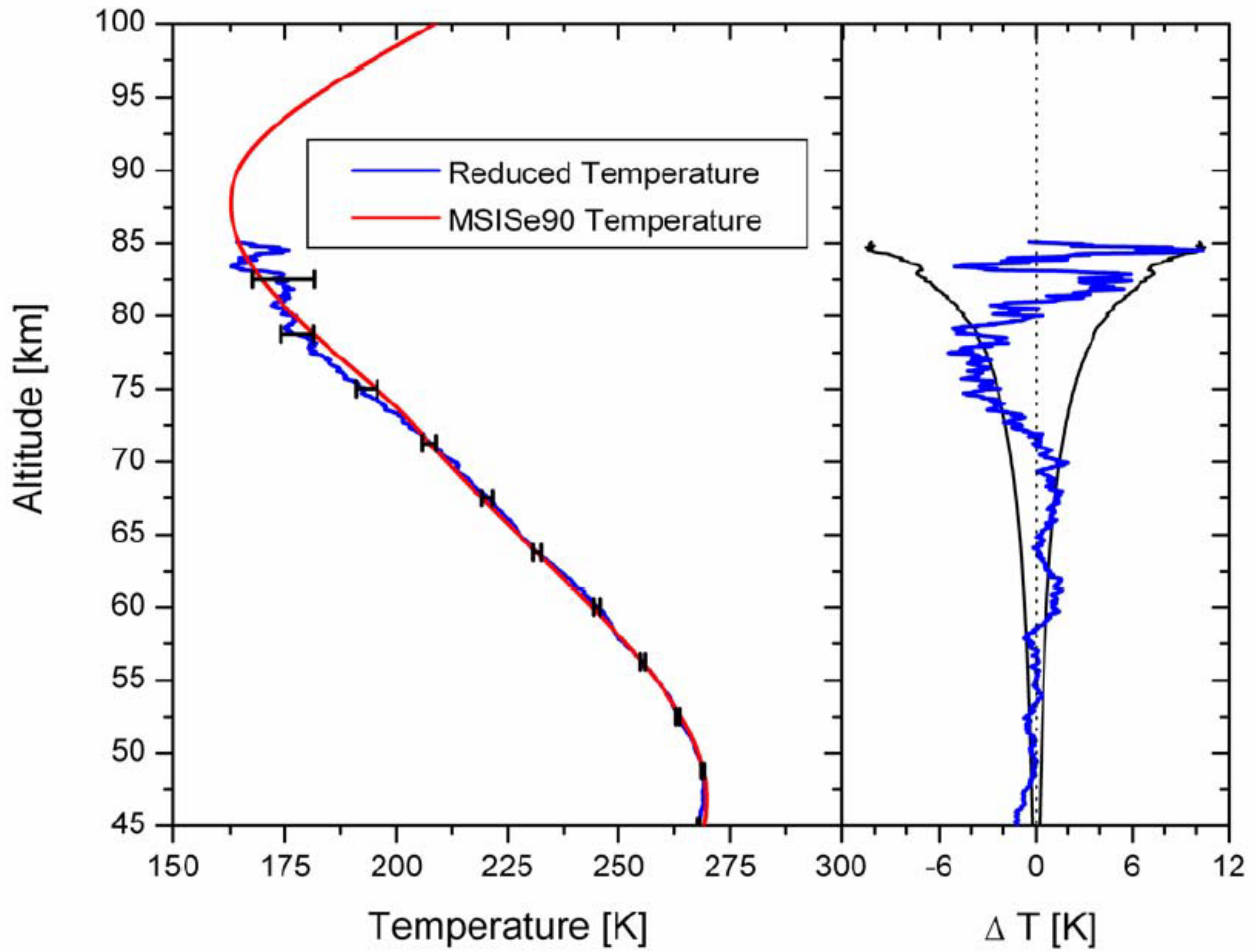

Courtesy of Josh Herron and Prof. Vincent Wickwar @ USU

Raman Scattering of N_2 and O_2

532 nm

607 nm

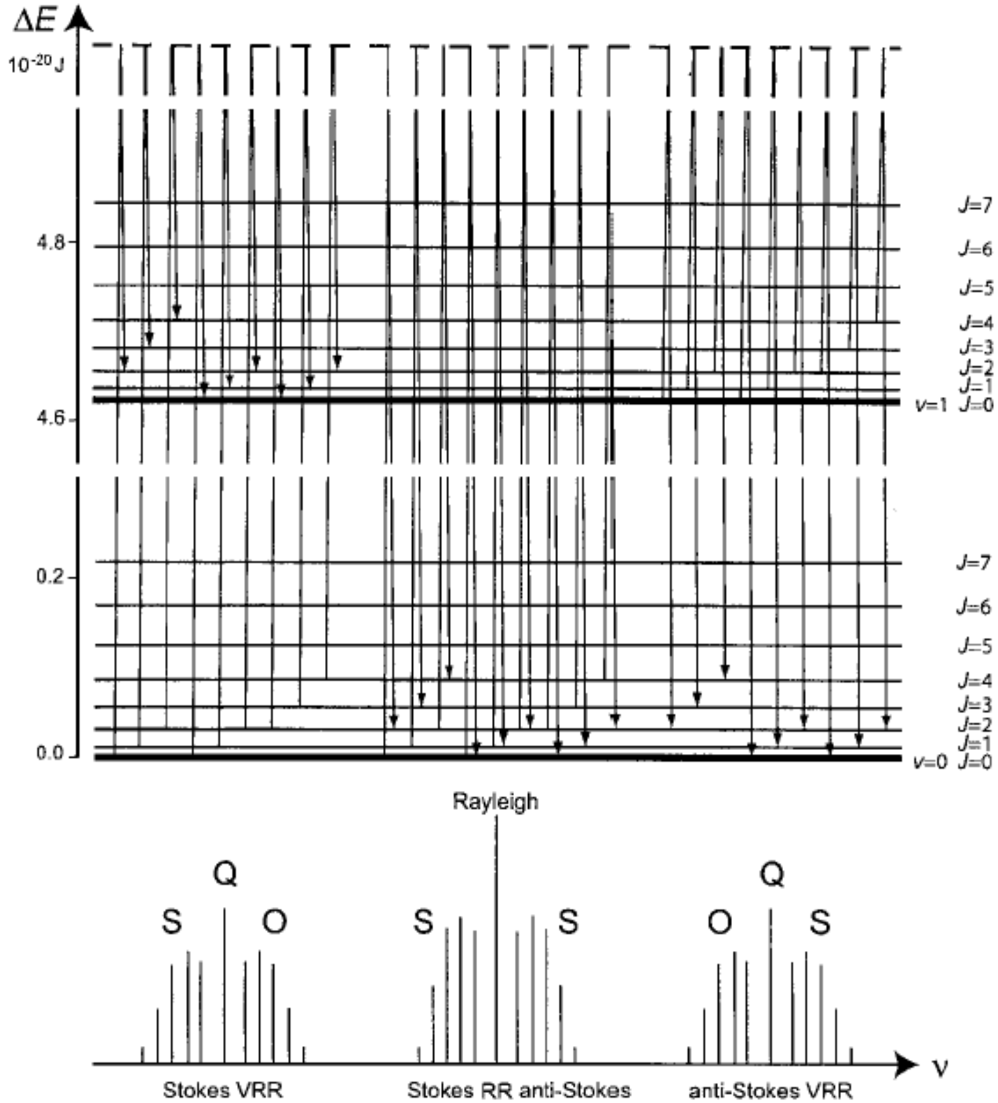

Fig. 9.1. Vibration–rotation energy levels of the N_2 molecule, Raman transitions, and resulting spectrum.

355 nm

387 nm

- Raman shift amount is independent of incident laser wavelength

Raman Integration Lidar

- In the lower atmosphere region where aerosols present Rayleigh scattering returns are contaminated by aerosol Mie scattering, so cannot be used in the integration technique.
- However, Raman scattering only comes from molecules, thus, free of aerosol influence. By detecting Raman scattering at a different wavelength (e.g., 607 nm compared to 532 nm), Mie and Rayleigh contamination are avoided.

$$N_S(\lambda,\lambda_L,z) = \left(\frac{P_L(\lambda_L)\Delta t}{hc/\lambda_L}\right)\left(\sigma_{Raman}(\lambda_L,\lambda,z)n_{N_2}(z)\Delta z\right) \times \left(\frac{A}{z^2}\right) T_a(\lambda_L,z)T_a(\lambda,z)\left(\eta(\lambda_L)\eta(\lambda)G(z)\right) + N_B$$

Lidar Backscatter Ratio ⇒ Relative Density ⇒ Temperature
(at different altitudes) (Raman)

Rayleigh-Raman Integration Lidar

[Keckhut et al., 1990]

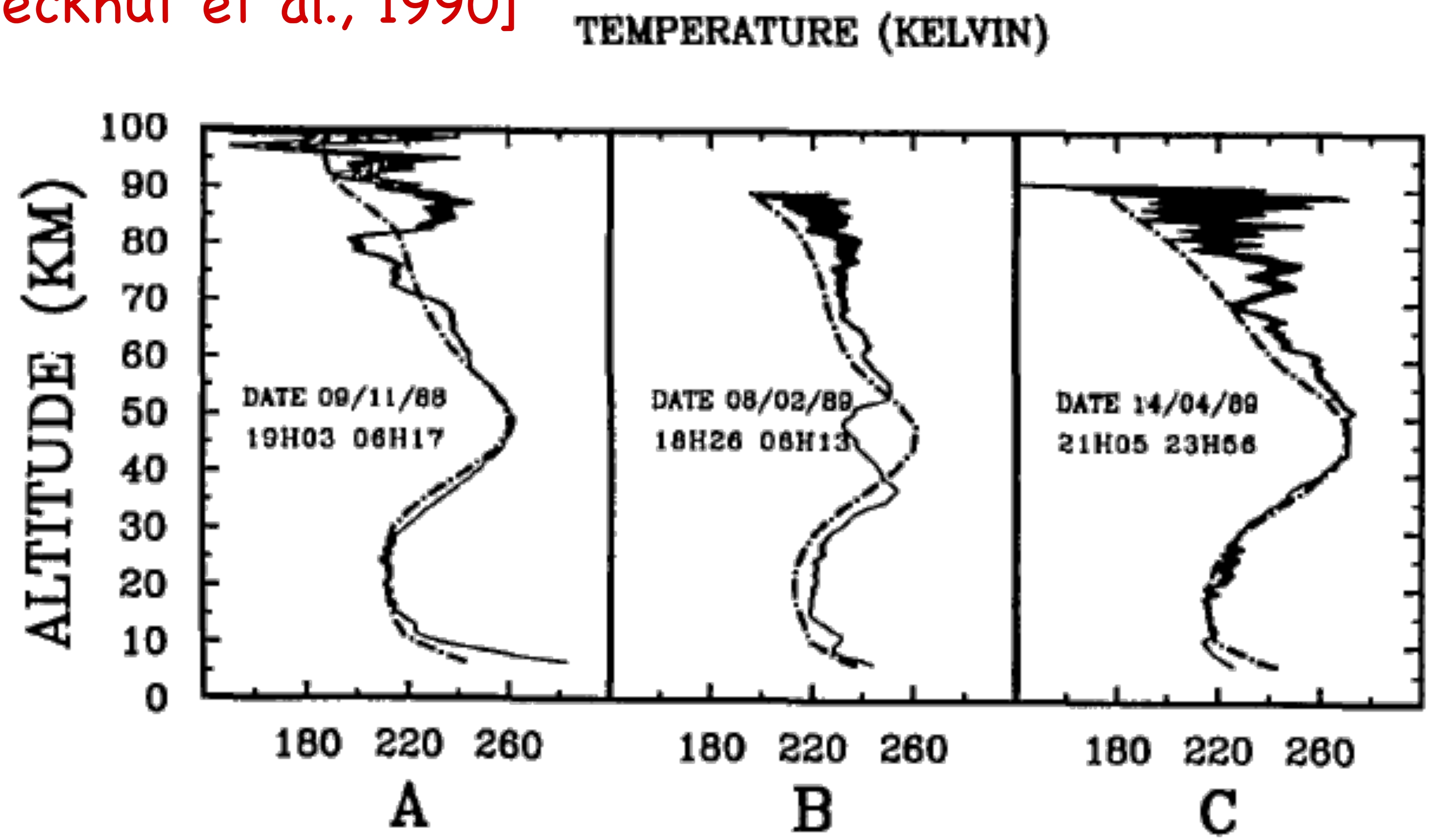

Fig. 2. Lidar temperature profiles compared with the corresponding CIRA 1988 model (dashed lines): (A) 09/11/88, 19H03 06H17; (B) 08/02/89, 18H26 06H13; (C) 14/04/89, 21H05 23H56.

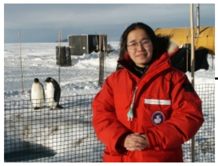

Inflatable Falling Sphere

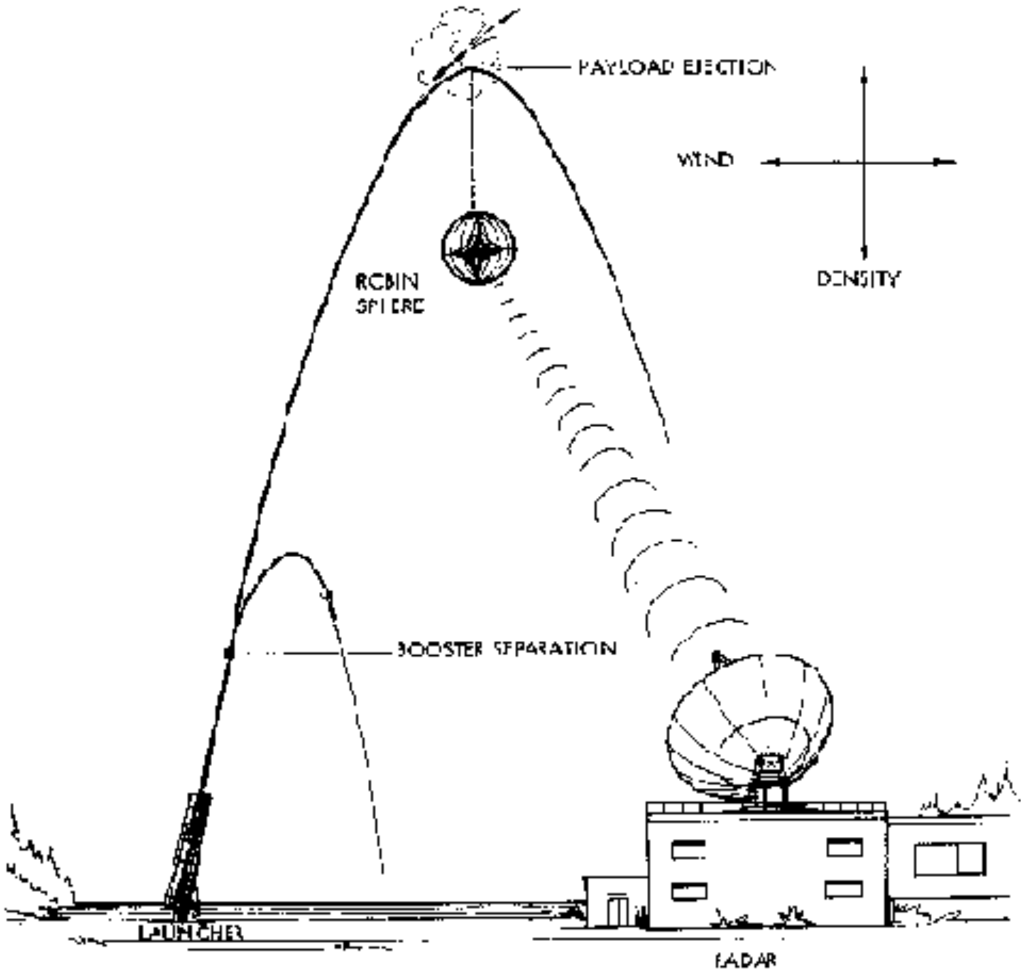

Bollerman and Walker, 1983

Rocket transports a metal sphere to upper atmosphere

⇩

After release the sphere inflates to 1-m metal sphere falling through atmosphere

⇩

High-precision radar tracks sphere position & acceleration

⇩

Input to the equation of motion of the falling sphere to derive atmosphere density

⇩

Integration from top to derive temperature from density data

[Schmidlin et al., JGR, 96(D12), 22673-22682, 1991]

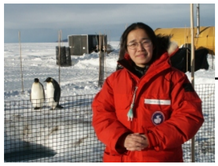

Falling Sphere Temperature

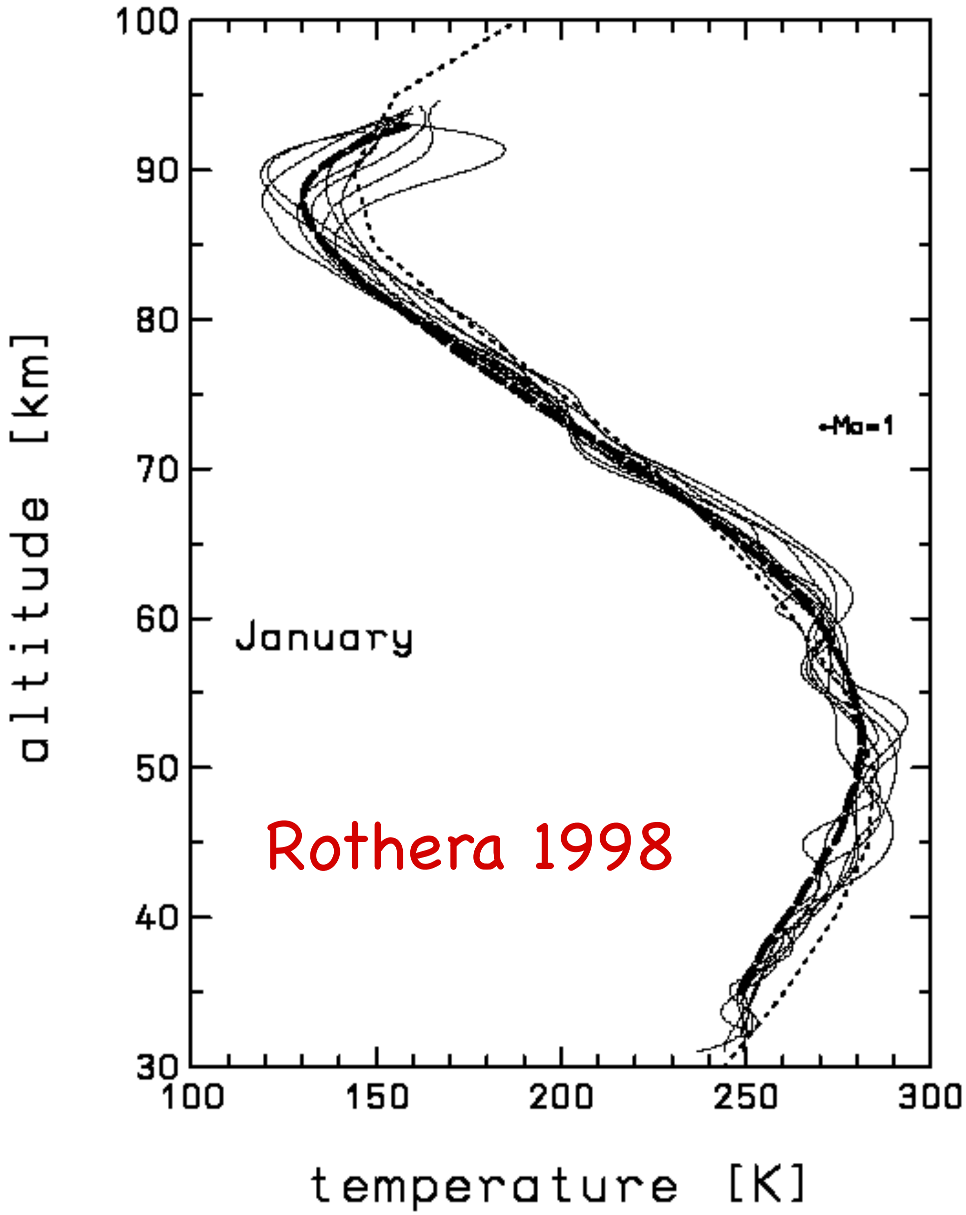

Rayleigh/Raman Lidar Instrumentation

- Typical Rayleigh/Raman temperature lidar utilizes the commercial Nd:YAG laser system as it provides robust laser power and operation (usually broadband).
- Any (short wavelength) resonance fluorescence lidar, like Fe Boltzmann lidar, also functions as a Rayleigh lidar in the region free of aerosol and fluorescence (about 30-75 km).
- Rayleigh scattering is inversely proportion to the 4th power of wavelength. So the shorter the wavelength, the stronger the Rayleigh scattering, as long as atmosphere absorption is not too strong.
- Operating in deep Fraunhofer lines will benefit daytime operation to reduce the solar background.
- Availability and robustness of laser systems are another consideration in lidar design.

Fe Boltzmann/Rayleigh Lidar

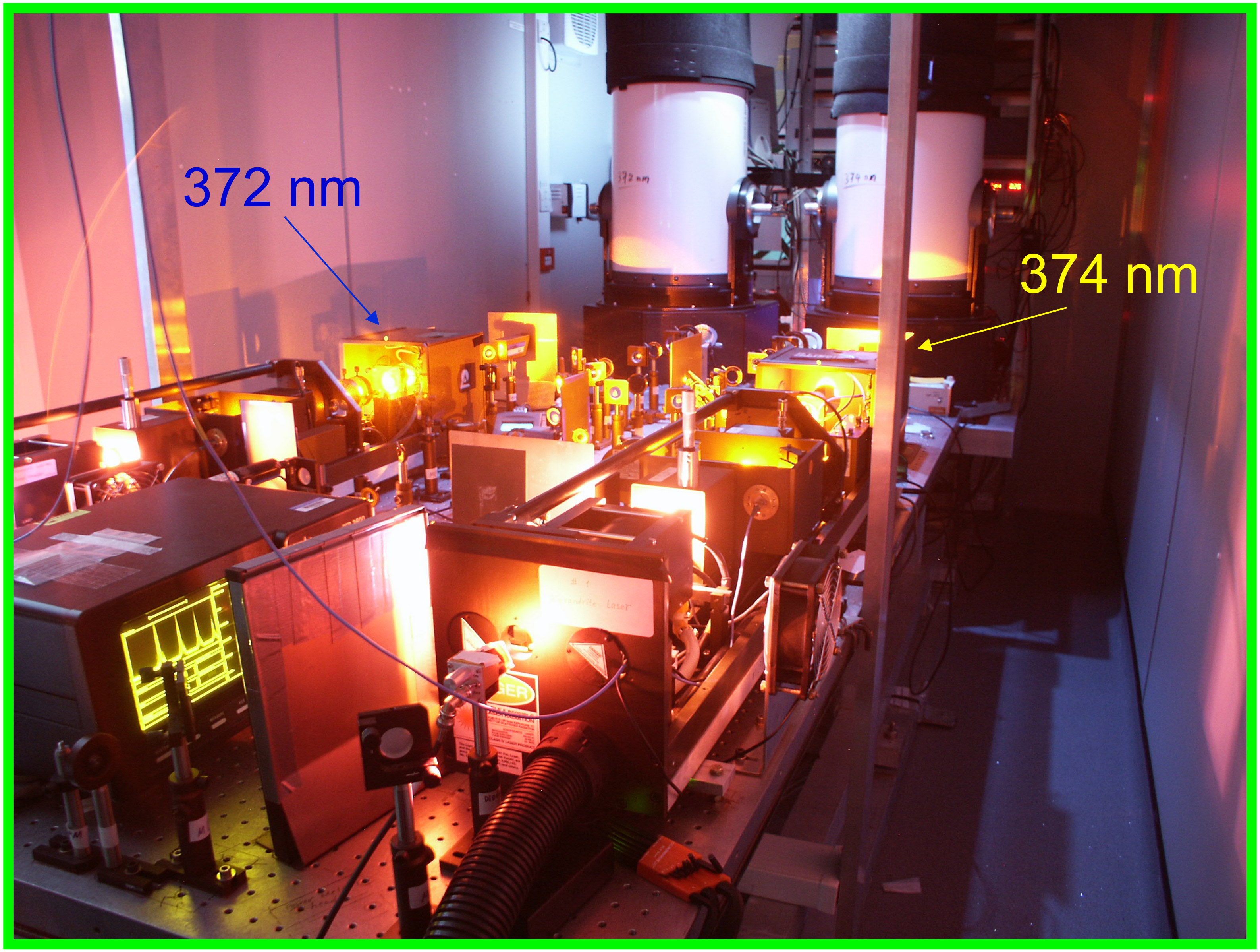

Sample Results from Fe Boltzmann/Rayleigh Lidar

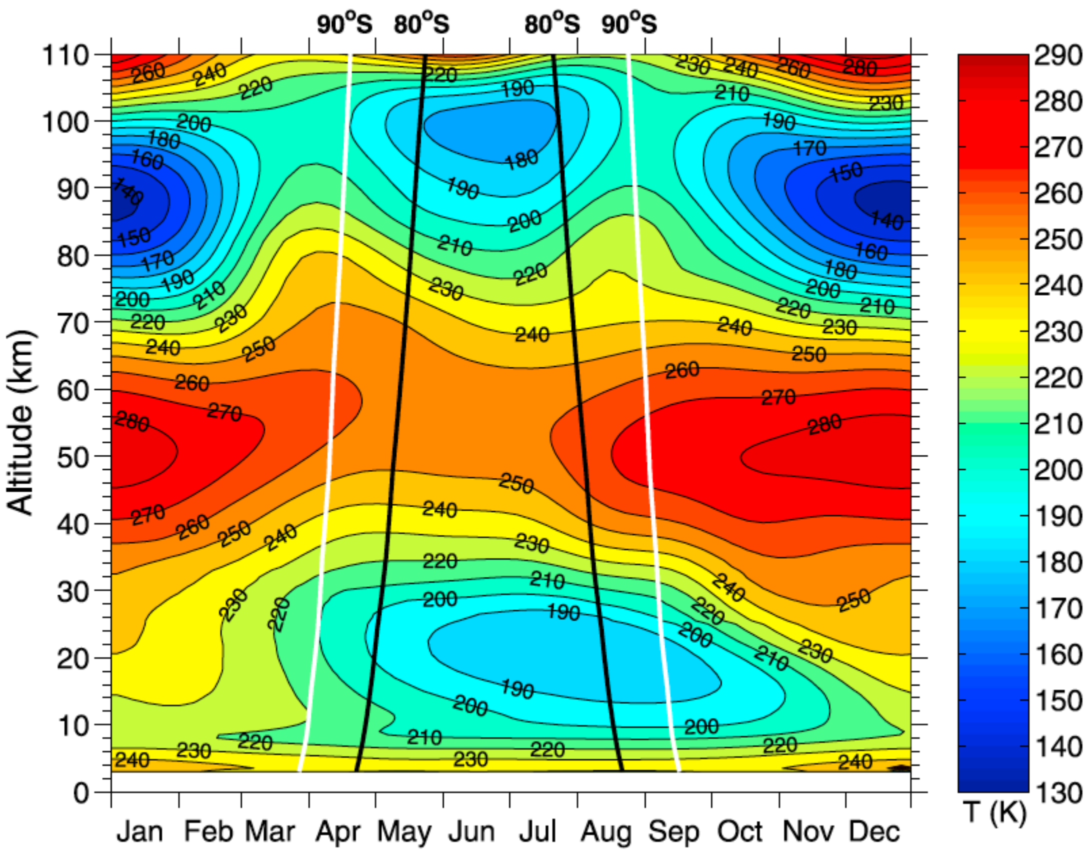

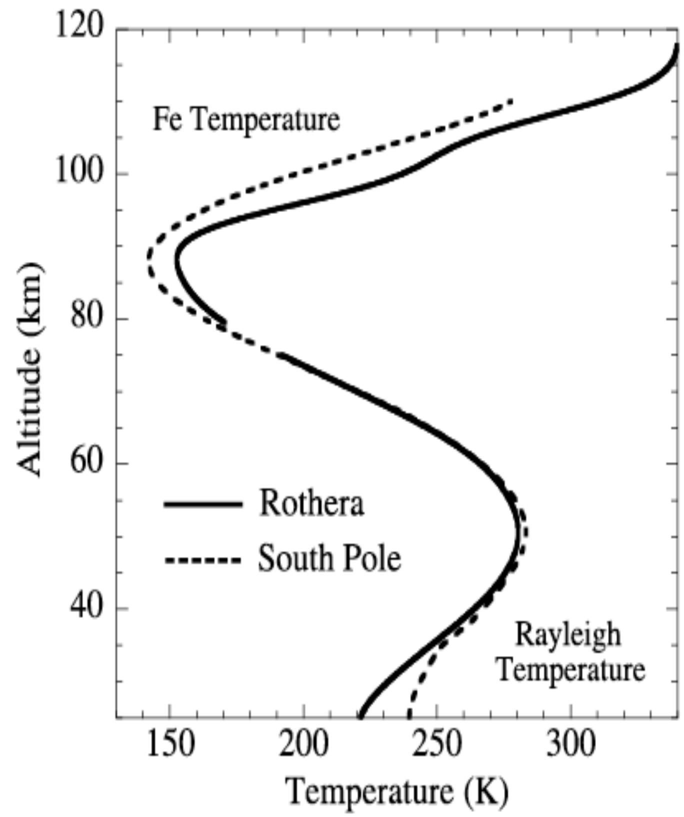

Figure 4. The observed weekly mean temperature structure of the atmosphere above South Pole (UISP-02) plotted from 3 to 110 km. Polar nights (24 h darkness) occur between the white curves at 90°S and between the black curves at 80°S. The vertical resolution is 500 m.

Utah State University Rayleigh Lidar

- Doubled Nd:YAG laser at 532 nm (630 mJ/pulse, 30 Hz)

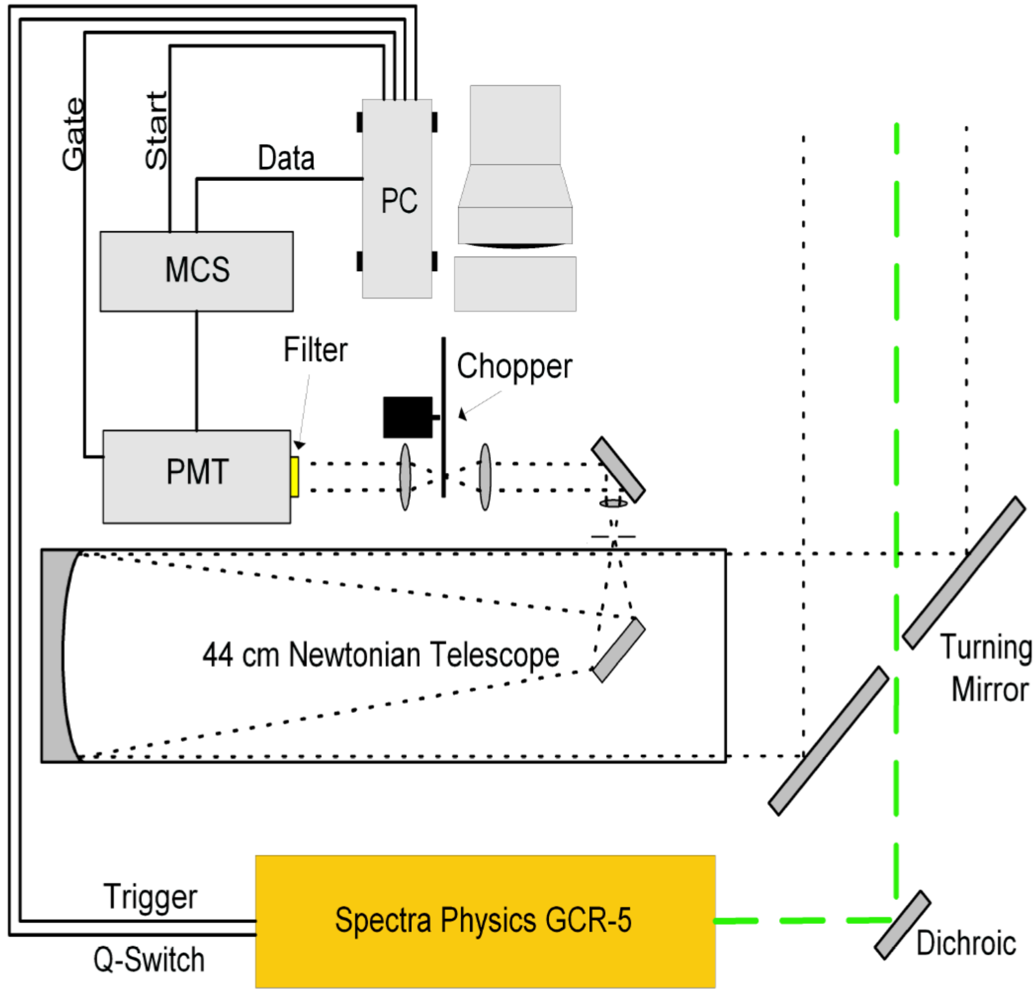

http://www.usu.edu/alo/aboutlidar.htm

Sample Results from USU Rayleigh Lidar

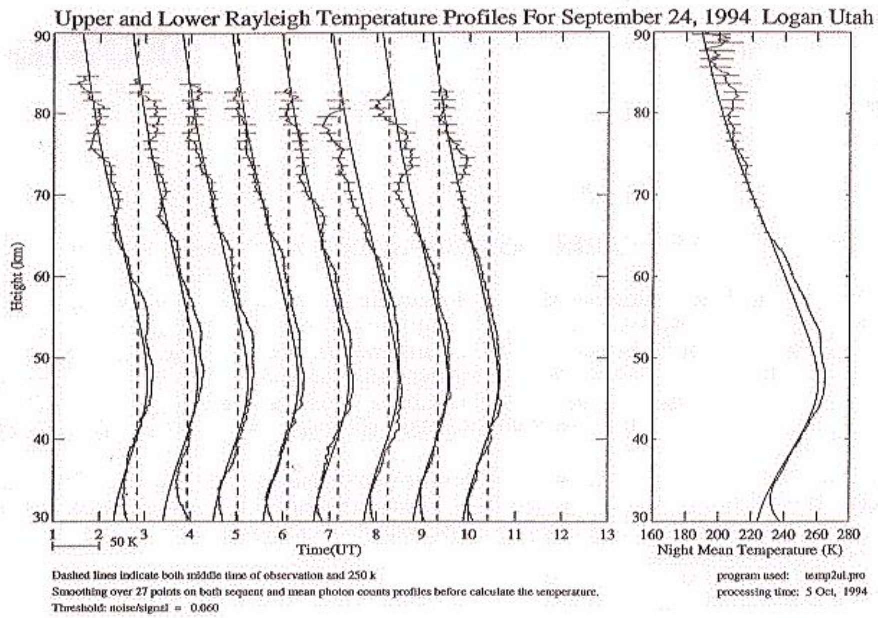

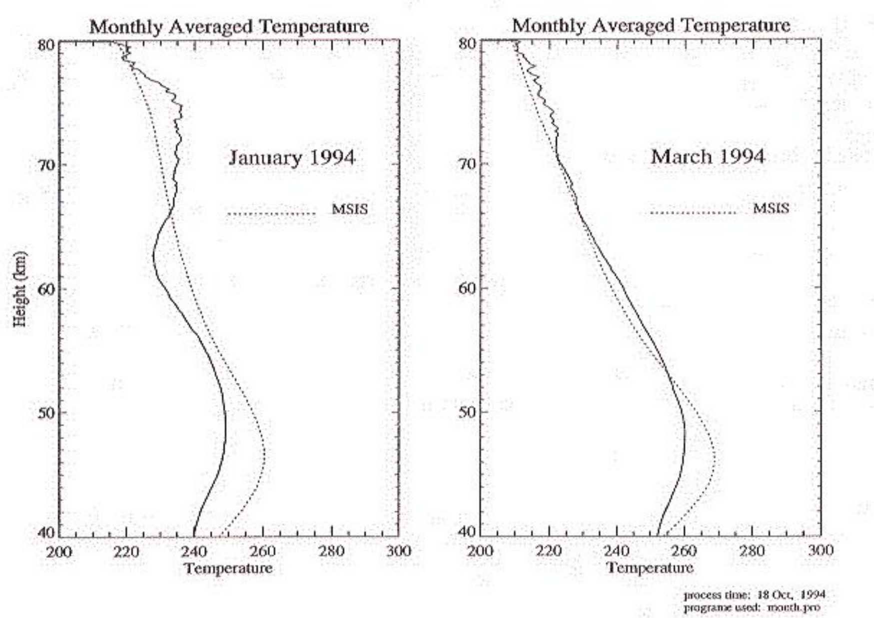

Prof. Vincent Wickwar
& Josh Herron @ USU

http://www.usu.edu/alo/aboutlidar.htm

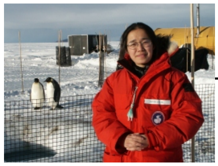

Greenland Rayleigh Lidar and Sample Results

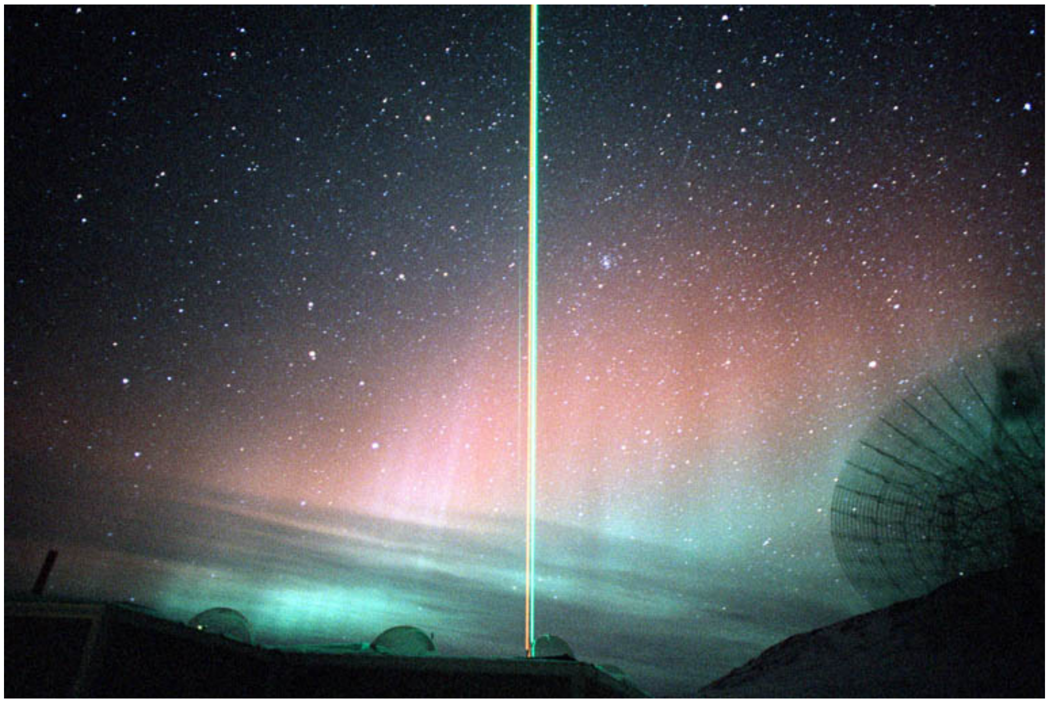

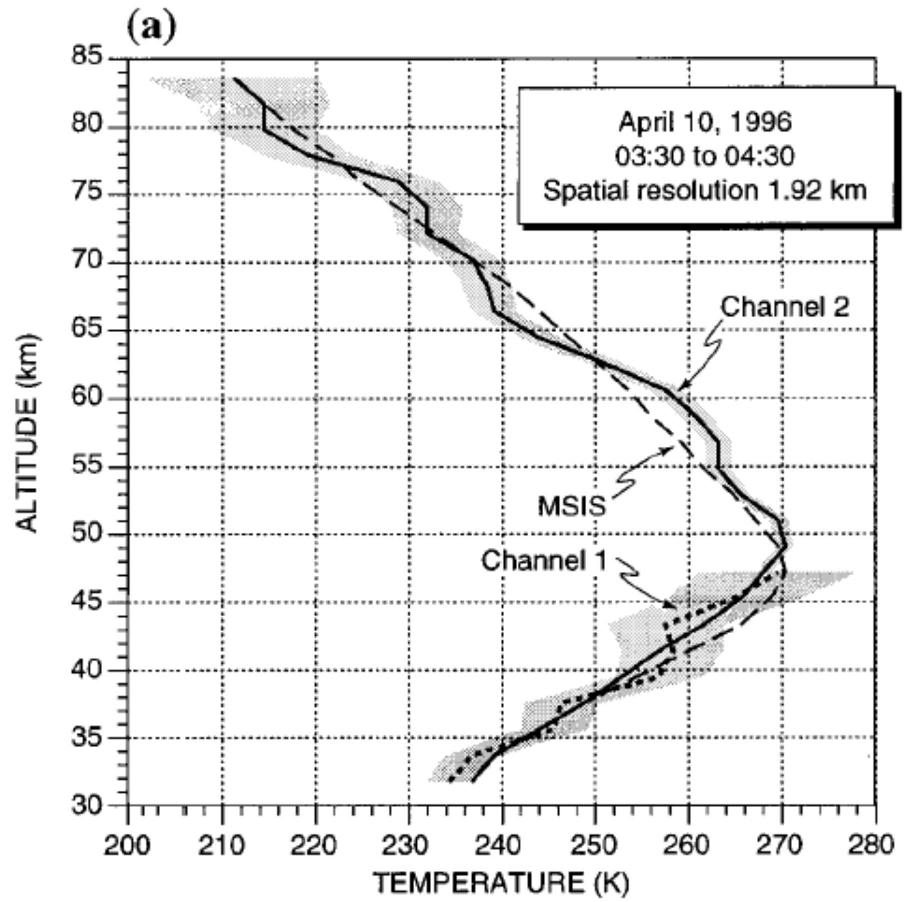

Courtesy of Jeff Thayer

Greenland Rayleigh Lidar System

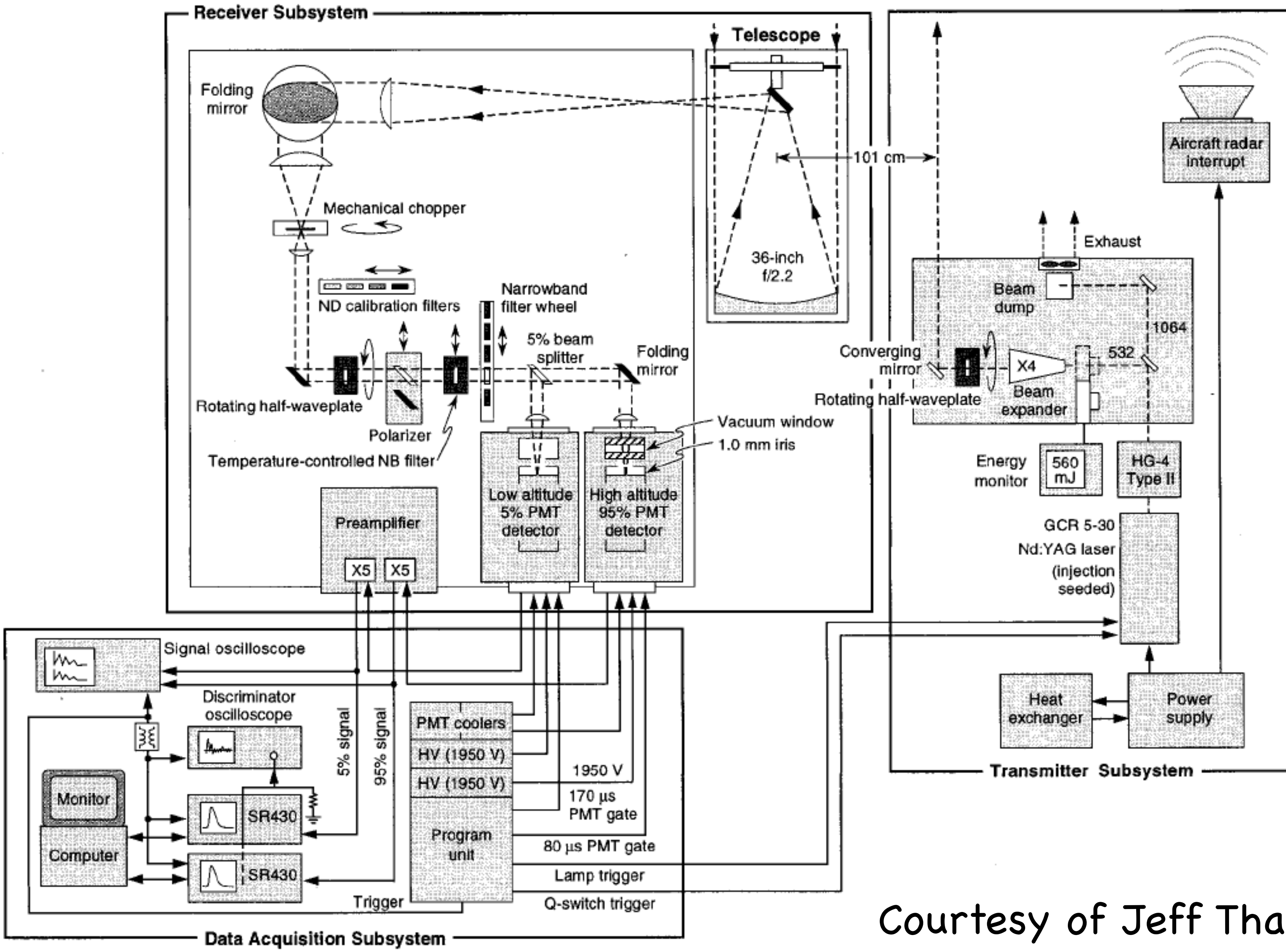

Courtesy of Jeff Thayer

Summary

- Integration technique relies on the assumptions of hydrostatic equilibrium and ideal gas law in the atmosphere interested. It involves integrating the atmosphere relative density profile downward using a starting temperature (usually coming from a model or independent measurement) at an upper altitude.
- The key is to somehow measure the atmosphere relative number density with high precision and unbiased.
- Integration technique started with cw searchlight in 1950s, dramatically enhanced by high-power pulsed Rayleigh lidar in 1980s for region free of aerosols, further developed by vibrational Raman lidar in 1990s for region with aerosols.
- Inflatable falling sphere released by rocket is another perfect example for integration temperature technique.